

## AN ERROR ANALYSIS OF THE GEOMETRIC BAADE-WESSELINK METHOD

MASSIMO MARENGO, MARGARITA KAROVSKA, AND DIMITAR D. SASSELOV

Harvard-Smithsonian Center for Astrophysics, 60 Garden Street, Cambridge, MA 02138; mmarengo@cfa.harvard.edu,  
mkarovska@head-cfa.harvard.edu, sasselov@cfa.harvard.edu

AND

MAYLY SANCHEZ

Department of Physics, Harvard University, 17 Oxford Street, Cambridge, MA 02138; msanchez@physics.harvard.edu

Received 2003 March 31; accepted 2003 November 12

### ABSTRACT

We derive an analytic solution for the minimization problem in the geometric Baade-Wesselink method. This solution allows deriving the distance and mean radius of a pulsating star by fitting its velocity curve and angular diameter measured interferometrically. The method also provides analytic solutions for the confidence levels of the best-fit parameters and accurate error estimates for the Baade-Wesselink solution. Special care is taken in the analysis of the various error sources in the final solution, among which are the uncertainties due to the projection factor, the limb darkening, and the velocity curve. We also discuss the importance of the phase shift between the stellar light curve and the velocity curve as a potential error source in the geometric Baade-Wesselink method. We finally discuss the case of the classical Cepheid  $\zeta$  Gem, applying our method to the measurements derived with the Palomar Testbed Interferometer. We show how a careful treatment of the measurement errors can be used to discriminate between different models of limb darkening by using interferometric techniques.

*Subject headings:* Cepheids — stars: fundamental parameters — stars: individual ( $\zeta$  Geminorum) — stars: oscillations — techniques: interferometric

### 1. INTRODUCTION

Since its conception, the Baade-Wesselink (BW) method (Baade 1926; Wesselink 1946) has been adopted as a preferred way to measure the distance of pulsating stars. In its classical formulation, the distance modulus of a star is derived from the stellar physical radius, obtained by integrating the stellar radial velocity curve, and its effective temperature. The method has been applied to calibrate the period-luminosity relation for different classes of pulsators, among which are RR Lyrae stars (McDonald 1977; Jones et al. 1992; Cacciari, Clementini, & Fernley 1992; Fernley 1994; Bono, Caputo, & Stellingwerf 1994), Cepheids (see review by Gautschi 1997), and  $\delta$  Scuti and SX Phoenix variables (Meylan et al. 1986).

The main limitation of this technique, however, consists in finding a reliable observable yielding an accurate estimate of the stellar  $T_{\text{eff}}$  (Böhm-Vitense et al. 1989). As a result, many variants of the BW method have been developed to circumvent this problem, by using different combinations of colors and bandpasses (see, e.g., Gieren, Barnes, & Moffett 1993; Laney & Stobie 1995; Riipei et al. 1997; Balog, Vinkó, & Kaszás 1997). Despite these ongoing observational efforts, discrepancies in the BW distances derived with different colors are still present (Laney & Stobie 1995; Krockenberger, Sasselov, & Noyes 1997).

Recent progress in interferometric techniques has made possible direct determination of angular diameter variations in nearby pulsating stars. This achievement has resulted in the development of a *geometric* version of the Baade-Wesselink method, which is in principle free of the limitations of the color-based techniques. Applied to the Galactic Cepheids, this method should eventually lead to a reliable zero point of the Cepheid distance scale (Sasselov & Karovska 1994).

Attempts to measure the angular radial displacements of pulsating Cepheids were made using the IOTA interferometer (Kervella et al. 2001), the Palomar Testbed Interferometer (PTI; Lane, Creech-Eakman, & Nordgren 2000; Lane et al. 2002), and the Naval Prototype Optical Interferometer. The results of these observations show that the BW method can indeed be used to yield distances of nearby Cepheids with a much better accuracy than other methods, including geometric parallax (Feast & Catchpole 1997; ESA 1997).

The geometric BW method is limited in its accuracy by uncertainties due to observational errors and model dependencies. These model dependencies derive from the need to translate the observed visibilities into angular diameters, which require accurate center-to-limb brightness profiles specific for the pulsating star. These profiles can be derived from hydrodynamic models of the stellar atmosphere (Marengo et al. 2002, hereafter Paper I). The conversion of radial velocities into radial displacement requires the knowledge of a projection factor, which is computed by modeling line formation in the pulsating atmosphere (Sabbey et al. 1995). To these model-dependent uncertainties one should add the intrinsic errors of the interferometric measurements and possible irregularities in the periodic pulsational behavior of the star.

In this paper we revisit the geometric BW method in order to discuss the relative importance of various uncertainties, assessing their contribution to the accuracy of the final distance determination. We first derive an original analytical solution for the BW method fitting procedure, which simplifies the determination of the best-fit distance and average radius from the observational data and allows a more transparent analysis of the individual error sources. We then apply our revised method on  $\zeta$  Gem PTI data (Lane et al. 2002), and we conclude with a discussion of the importance of the errors

due to the pulsational model uncertainties (projection factor and limb darkening) and the phase shift between the light curve of the pulsator and the dynamical phases of the radial velocities.

## 2. GEOMETRIC BAADE-WESSELINK METHOD

The *geometric* BW method allows one to derive the distance and the mean radius of a pulsating star by fitting the variations of its angular diameter measured interferometrically, with the radial displacement  $\Delta R(\phi)$  of the stellar photosphere. The radial displacement is in turn derived by integrating the pulsational velocity over time:

$$\Delta R(\phi) = \int_{\phi_0}^{\phi} p(\phi') [v_r(\phi') - \gamma] d\phi', \quad (1)$$

where  $v_r(\phi)$  is the radial velocity, which should be corrected for the systemic velocity  $\gamma$  and the projection factor  $p(\phi)$  to yield the pulsational velocity.

As explained in Paper I the systemic velocity is calculated by requiring the conservation of the radius over one period. It takes into account the radial motion of the star relative to the solar system and physical inconsistencies in the measurement of the radial velocities with spectral data. An appropriate  $p$ -factor is computed by modeling spectral line formation for a given pulsating star, including spectral line asymmetries and the dynamics of the pulsation. Models for several classical Cepheids have been computed by Sabbey et al. (1995), from which the pulsational phase-dependent  $p$ -factors are derived. The variations of the radial velocity with the pulsational phase are instead measured spectroscopically. A recent compilation of radial velocity data for 40 Cepheids has been published by Bersier et al. (1994b), by using the CORAVEL spectrophotometer. The measurements are provided as a Fourier expansion of  $v_r$ , in terms of the pulsational phase  $\phi$ . The integration of the  $v_r(\phi)$  curve provides the required radial displacement  $\Delta R(\phi)$ , used in combination with the measured angular diameters in the geometric BW method.

The BW distance  $D$  and average radius  $R_0$  of the pulsating star are solved as a two-parameter  $\chi^2$  minimization:

$$\chi^2(R_0, D) = \sum_i \left( \frac{\Theta_i - \theta_i}{\sigma_i} \right)^2 = \sum_i \left\{ \frac{2[(R_0 + \Delta R_i)/D] - \theta_i}{\sigma_i} \right\}^2, \quad (2)$$

where the index  $i$  runs on the data points,  $\theta_i$  is the angular diameter measured at a certain phase  $\phi_i$ , and  $\Delta R_i = \Delta R(\phi_i)$  is the radial displacement derived with equation (1) for the same phase. The terms  $\sigma_i$  are the errors associated with each data point, including the uncertainty in the radial displacement. Note that when converting the time of each individual data point  $\theta_i$  into the pulsational phase  $\phi_i$  of the radial displacement curve, one must take special care to take into account the phase shift observed between the stellar light curve and the radial velocity curve from which  $R(\phi_i)$  is derived. Note also that the diameters  $\theta_i$ , when measured with an interferometer, should consider the limb darkening (LD) of the stellar atmosphere. As in the case of the  $p$ -factor, this quantity is also affected by the stellar pulsation and depends on the pulsational phase. In Paper I a method was presented to compute wavelength and phase-dependent LD by using the same hydrodynamic models from which the Sabbey et al. (1995)  $p$ -factor was derived.

The  $\chi^2$  fit for the geometric BW method is solved by minimizing equation (2) with respect to the average radius  $R_0$  and the distance  $D$ . The minimum  $\chi^2$  is found at the stationary point of  $\chi^2(R_0, D)$ :

$$\partial_{R_0} \chi^2 = 0, \quad \partial_D \chi^2 = 0, \quad (3)$$

which gives a system of two linear equations in  $D$  that are quadratic in  $R_0$ :

$$D = \frac{2A}{B} R_0 + \frac{2C}{B}, \quad D = 2 \frac{AR_0^2 + 2CR_0 + F}{BR_0 + E}, \quad (4)$$

where the following coefficients are defined as

$$\begin{aligned} A &= \sum_i \frac{1}{\sigma_i^2}, & B &= \sum_i \frac{\theta_i}{\sigma_i^2}, \\ C &= \sum_i \frac{\Delta R_i}{\sigma_i^2}, & E &= \sum_i \frac{\Delta R_i \theta_i}{\sigma_i^2}, \\ F &= \sum_i \frac{\Delta R_i^2}{\sigma_i^2}, & G &= \sum_i \frac{\theta_i^2}{\sigma_i^2}. \end{aligned} \quad (5)$$

The system in equation (4) describes two curves intersecting at the minimum  $\chi^2$ . The angular coefficient of the first curve, which is a first-order polynomial, is  $2A/B$ . The second curve, when linearized to the first order, has an angular coefficient also very close to  $2A/B$ . This means that the two curves described by the system in equation (4) are almost parallel. Their intersection will thus result in a large uncertainty along the  $D/R_0 = 2A/B$  direction and a much smaller error in the orthogonal direction.

The system in equation (4) can be solved by direct substitution, obtaining first an explicit solution for  $R_0$  in terms of the coefficients defined in equation (5). When the solution for  $R_0$  is substituted back into the second equation, the quadratic terms cancel, leaving a unique solution for  $D$ . Thus, the best-fit distance  $\bar{D}$  and mean radius  $\bar{R}_0$  are

$$\bar{R}_0 = \frac{CE - BF}{BC - AE}, \quad \bar{D} = 2 \frac{BC^2 - ABF}{B^2C - ABE}. \quad (6)$$

The value of the  $\chi^2$  for the best-fit parameters is obtained by substituting  $\bar{R}_0$  and  $\bar{D}$  into equation (2), obtaining the following expression:

$$\begin{aligned} \chi_{\min}^2 &= \left| \chi^2(R_0, D) \right|_{\substack{R_0=\bar{R}_0 \\ D=\bar{D}}} \\ &= \left[ 4A \left( \frac{R_0}{D} \right)^2 + 8C \frac{R_0}{D^2} + 4 \frac{F}{D^2} - 4B \frac{R_0}{D} - 4 \frac{E}{D} + G \right]_{\substack{R_0=\bar{R}_0 \\ D=\bar{D}}}. \end{aligned} \quad (7)$$

The error region for the best-fit solution is determined by the confidence levels of the  $\chi^2(R_0, D)$ . Assuming a Gaussian error distribution, the 68% confidence level (giving the 1  $\sigma$  error) is defined by the equation

$$\chi^2(R_0, D) = \chi_{\min}^2 + \chi_{68\%}^2, \quad (8)$$

where  $\chi_{68\%}^2 = 2.33$  for a two-parameter fit (see, e.g., Frodesen, Skjeggstad, & Tofte 1979). The explicit form of the error contour in terms of  $R_0$  and  $D$  is obtained from equation (7) by substitution of  $\chi_{\min}^2$  with  $\chi_{\min}^2 + \chi_{68\%}^2$ . Note that the equation

describes a tilted ellipse having the major axis oriented along  $D = R_0$ .

Error bars for the  $R_0$  and  $D$  best-fit solution, at a certain confidence level, can be obtained analytically by determining the intersection of the error ellipse with appropriate lines parallel to the  $R_0$  and  $D$  axis. Each line intersects the ellipse at two points (given by a quadratic equation). The intersections that provide the error bars are the ones where these two points coincide; there are two such intersections for each axis, each of them given by the solution of a quadratic equation in  $D$  and  $R_0$ , respectively. These solutions can be solved explicitly in terms of the coefficients defined in equation (5) as

$$X^\pm = \pm \bar{X} \pm \frac{\pm \beta_X - \sqrt{\beta_X^2 - \alpha_X \gamma_X}}{\alpha_X}, \quad (9)$$

where  $X$  is either  $D$  or  $R_0$  and where the numeric coefficients in the two cases are

$$\begin{aligned} \alpha_D &= B^2 - AG + A(\chi^2 + \chi_{68\%}^2), \\ \beta_D &= 2(AE - CB), \quad \gamma_D = 4(C^2 - AF), \end{aligned} \quad (10)$$

and

$$\begin{aligned} \alpha_{R_0} &= B^2 - AG + A(\chi^2 + \chi_{68\%}^2), \\ \beta_{R_0} &= BE + C(\chi^2 + \chi_{68\%}^2) - CG, \\ \gamma_{R_0} &= E^2 + F(\chi^2 + \chi_{68\%}^2) - FG. \end{aligned} \quad (11)$$

The best-fit angular diameter is simply obtained as  $\bar{\Theta}_0 = \bar{R}_0/\bar{D}$ . Note that the expression for  $\Theta = R_0/D$  is the equation for the major axis of the error ellipse. Lines parallel to the ellipse major axis are the regions of constant angular size for the generic  $R_0$  and  $D$  solutions; the error bars for  $\bar{\Theta}_0$  are thus given by the intersections of these lines with the error ellipse. The solution can then be found analytically, as in the case of the error bars of  $R_0$  and  $D$ , with the following coefficients:

$$\begin{aligned} \alpha_{\Theta_0} &= C^2 - AF, \quad \beta_{\Theta_0} = BF - CE, \\ \gamma_{\Theta_0} &= E^2 + F(\chi^2 + \chi_{68\%}^2) - FG. \end{aligned} \quad (12)$$

### 3. APPLICATION TO THE CLASSICAL CEPHEID $\zeta$ GEM

To illustrate the procedure described in the previous section and analyze the relative importance of the various error sources in the final solution, we can consider the case of the classical Cepheid  $\zeta$  Gem, recently observed with the PTI interferometer (Lane et al. 2002). The uniform disk (UD) angular diameters  $\theta_i^{(UD)}$  obtained for  $\zeta$  Gem in the near-IR  $H$  band using the PTI have been published in Table 4 of Lane et al. (2002). Each diameter results from a number of individual measurements (scans) performed on a certain Julian Date (JD). The JD of each measurement is converted into the  $\zeta$  Gem light-curve phase  $\phi_L^{(i)}$  by using the published period  $P = 10.150079$  days and the zero-phase epoch  $T_0 = 2,444,932.736$  (Lane et al. 2002). As mentioned previously, the fitting procedure requires reconciling the ‘‘dynamical’’ phase  $\phi_V$  of the radial velocity curve with the light-curve phase  $\phi_L$  of the observations. This is done by correcting for

the phase shift  $\Delta\phi = \phi_L - \phi_V$  observed between the maximum luminosity and the minimum radius. From the data collected by Bersier, Burki, & Burnet (1994a) and Bersier et al. (1994b) we derive  $\Delta\phi \simeq 0.28$ . This is the value we use in the following discussion. Limitations of this approach for deriving the phase shift are discussed in § 3.1.

To derive an accurate distance with the geometric BW method, the angular diameter measurements  $\theta_i$  should be corrected for the LD. For clarity, however, we first solve the BW fit by using the published UD diameter, deferring the discussion of the effect of the LD, and the errors associated with it, to a separate section. For the same reason, we adopt the value of the  $p$ -factor of 1.43 used in Lane et al. (2002), which is the average value derived by Sabbey et al. (1995) over the  $\zeta$  Gem pulsational cycle, consistent with the model we adopted for computing the LD.

As discussed before, the terms  $\sigma_i$  are the errors associated with each data point. They are the geometric sum of the individual errors for each observation:

$$\sigma_i^2 = \left(\sigma_i^{(\theta)}\right)^2 + \left(\sigma_i^{(\Delta R/D)}\right)^2, \quad (13)$$

where  $\sigma_i^{(\theta)}$  is the error of the interferometric measurement and  $\sigma_i^{(\Delta R/D)}$  is the error related to the diameter variation. According to Lane et al. (2002) the errors in the interferometric PTI UD data vary between 0.01 and 0.06 mas (10%–60% of the predicted amplitude of  $\zeta$  Gem pulsations, of  $\sim 0.1$  mas), depending on the quality of each measurement. Note that these errors refer only to the determination of the UD diameters. When computing the *true* distance of the star by using the diameters corrected for the LD, we also take into account the errors involved in the LD correction.

An estimate of the error related to  $\Delta R/D$  is more difficult to obtain. The first component in this error is due to the uncertainty in the radial velocity measurement. From Bersier et al. (1994a) we get that the average error in the  $\zeta$  Gem velocity measurement is about  $0.4 \text{ km s}^{-1}$  over velocities up to  $\sim 20 \text{ km s}^{-1}$ , which takes into account possible irregularities in the pulsational behavior of the star. This is a relative error of up to  $\sim 2\%$  (when the velocity is maximum), which translates to a maximum uncertainty in the expected stellar radius variation of  $\sim 0.002$  mas for the predicted amplitude of the  $\sim 0.1$  mas  $\zeta$  Gem pulsation. Another contribution to this error is the uncertainty in the  $p$ -factor; we use the same value of  $1.43 \pm 0.06$  as Lane et al. (2002), which takes into account the variation of  $p(\phi)$  with the pulsational phase (Sabbey et al. 1995). This adds a further  $\sim 4\%$  relative uncertainty to the measured pulsation amplitude (equivalent to  $\sim 0.004$  mas). The total error associated with the  $\zeta$  Gem angular diameter variation because of the uncertainties in the  $\Delta R/D$  fitting function (again assuming that the two error sources are not correlated and add as their geometric sum) is thus  $\sim 4.5\%$ . This is equivalent to a maximum error of  $\sim 0.005$  mas for the predicted amplitude of the  $\zeta$  Gem pulsations. Note that this error, in general, is smaller than the error of the current interferometric data but may become important in the future, given the promising advances in the interferometric techniques. To include the  $\sigma_i^{(\Delta R/D)}$  in the BW fit, we have first solved equation (6) in order to have a preliminary estimate of  $D$  and then evaluated the  $\sigma_i^{(\Delta R/D)} \simeq 0.06 \Delta R_i/D$  for each point. Finally, considering both error sources, we have repeated the  $\chi^2$  fitting procedure.

The best-fit results are summarized in Figure 1, which shows the BW distance and average radius for the PTI UD

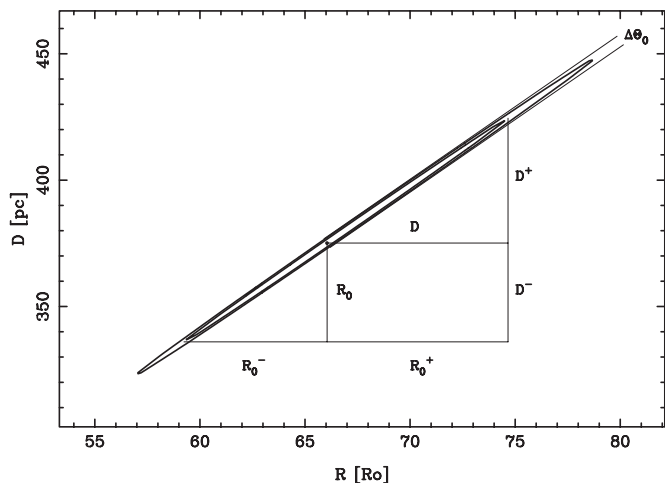


FIG. 1.—BW fit of  $\zeta$  Gem distance and mean radius from PTI  $H$ -band UD data. Inner contour is 68% confidence level ( $1\sigma$ ), and outer contour is 90% confidence level error.

data and the error regions for the 90% (*external oval*) and 68% (*inner oval*) confidence level. As expected, the error regions are ellipses with the major axis oriented along the  $R_0/D = \text{const}$  direction. The ellipses are very narrow, resulting in large errors, individually, in the best-fit  $R_0$  and  $D$  but a small error in their ratio  $\Theta_0 = R_0/D$ . This is not surprising, since the accuracy of the interferometric measurements is good enough to produce a reasonable fit to the average angular radius of the pulsating star; a much higher accuracy is instead required to measure the radial displacement, from which  $R_0$  and  $D$  are measured with the BW method. Equation (2) can in fact be written as

$$\chi^2 = \sum_i \left[ \frac{\Theta_0 + (2\Delta R_i/D) - \theta_i}{\sigma_i} \right]^2. \quad (14)$$

Given that the maximum angular diameter variations are less than 10% of the average angular diameter, then for most phases  $\Theta_0 \gg 2\Delta R_i/D$ . This means that the fit is essentially a one-parameter fit for  $\Theta_0$ , which can be determined with good accuracy. The measurement errors play a much larger effect in limiting the accuracy of  $R_0$  and  $D$  along  $R_0/D = \Theta_0$ .

### 3.1. Phase Shift Determination

Two basic questions remain open regarding the accuracy of the fit using the BW method. The first concerns the assumption that the phases of the interferometric data and radial velocities are well synchronized, e.g., that there is not an unknown phase shift component between the luminosity light curve and radial pulsations. The second question concerns the LD correction, which we need to apply to the UD measurement to derive the correct BW distance.

As mentioned before, the BW method requires defining a common phase reference for diameter observations and radial velocity data. This is usually provided by the light-curve phases  $\phi_L$ , with the zero phase set to coincide with the maximum luminosity. A complication can, however, arise when observable quantities are related to phase-dependent parameters that are derived from dynamic modeling of pulsating stars. Typical parameters are the  $p$ -factor (Sabbey et al. 1995) and the LD correction (Paper I). The traditional choice of the light-curve phase is not convenient when dealing with

time-dependent hydrodynamic models, e.g., the ones from which the  $p$ -factor and the LD are computed. The emergent flux in a given waveband is in fact a derived quantity (which can be computed only with extensive radiative transfer modeling) and is usually not available in hydrodynamic numeric computations. A better approach in this case is to choose the zero-phase reference based on hydrodynamic quantities directly tied with observables, such as the radial velocity  $v_r$ . This leads to the “dynamical phase”  $\phi_V$  mentioned before.

The complication in reconciling the light curve and dynamical phase references is due to the phase shifts occurring between the zero phases in the two systems. This quantity can be obtained by carefully measuring the light curve and velocity curve of the pulsating star, as done by Bersier et al. (1994a, 1994b). This procedure yields for  $\zeta$  Gem the quantity  $\Delta\phi \simeq 0.28$  used in the previous section; different values should be expected for different stars, since the phase shift is determined by the unique dynamics of the pulsator. A different approach was followed by Lane et al. (2002), in which the phase shift was derived as a separate quantity in the BW fit, on the assumption that having a third free parameter would produce a better agreement between the measured angular diameters and the radial displacement curve.

To assess the effects on the fit results by an independent determination of the phase shift, we repeated the BW fit of the  $\zeta$  Gem PTI UD diameters leaving this parameter free. The results are shown in Figure 2, where the best fit is plotted in

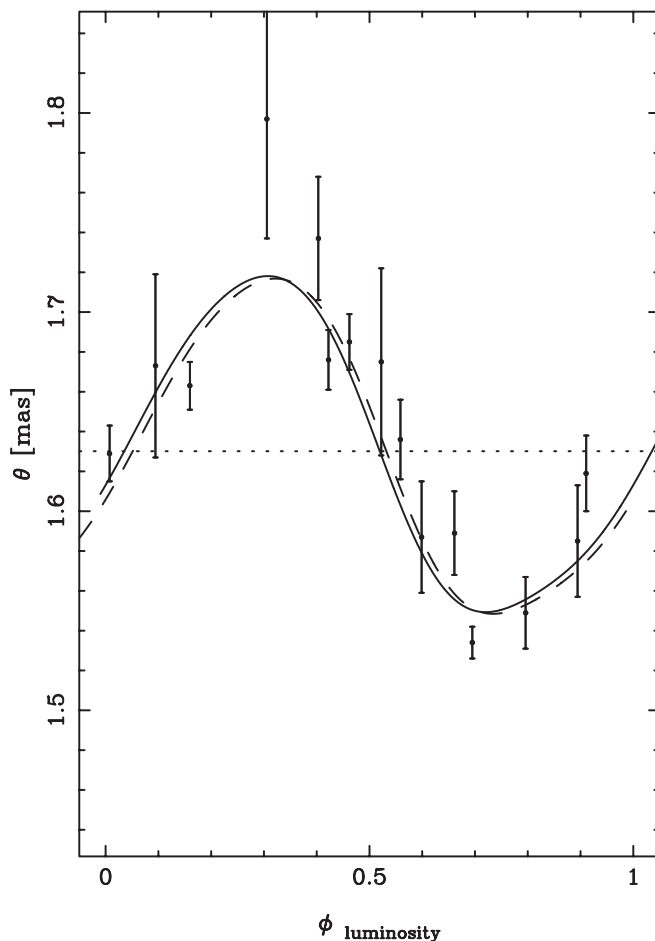


FIG. 2.—Best-fit UD diameter of  $\zeta$  Gem PTI  $H$ -band data from Lane et al. (2002). The solid line is the fixed phase shift as determined by Bersier et al. (1994a, 1994b). The dashed line is instead the best fit with the free phase shift.

the case of a free phase shift (*dashed line*), and a fixed phase shift (*solid line*) as determined from Bersier et al. (1994a, 1994b) data. The best-fit results with their errors are shown in Table 1.

The results show that the small difference in the phase shift, although “visually” improving the fit of the data points, does not change significantly the best-fit results. The difference in  $R_0$ ,  $D$ , and  $\Theta_0$  is well below the error bars resulting from the fit, which suggests that the shift itself can be a statistical deviation due to the uncertainties of the data points. It is, however, interesting to investigate the possible causes of this discrepancy, since an unaccounted-for phase shift would have profound implications in terms of the evolution of pulsating stars.

Since the actual phase of interferometric data acquired at a certain JD is determined by folding many pulsational periods starting from the zero-phase epoch, an uncertainty in the period determination can play a significant role in changing the measured phase shift. The typical uncertainty for the Cepheid periods tabulated in Bersier et al. (1994a) is on the order of  $\sim 10^{-4}$  days. The zero-phase epoch for  $\zeta$  Gem is around day 2,444,933, while the observations were made between JD 2,451,605 and 2,451,896. Clearly, the 300 day span in the time during which the observations were collected is not important since it corresponds to less than 30 periods. The time lag between the zero epoch and the data acquisition is on the other hand  $\sim 7000$  days, which is approximately 690 periods. Given the accuracy of the  $\zeta$  Gem period, the possible shift is on the order of  $\sim 0.07$  days. This is less than a 0.01 phase shift error, which is 1 order of magnitude less than the unaccounted-for phase shift derived by fitting the PTI data. Therefore, if the measured phase shift is real, it is not explained by the current uncertainty in the pulsational period.

Berdnikov et al. (2000) analyzed archival data of the maximum luminosity epochs for a number of classical Cepheids, in search of secular variations of their period due to evolutionary changes. In the case of  $\zeta$  Gem, they found a decrease of 0.07 days over a time of about 5000 pulsational cycles. This means a decrease of the period of  $1.4 \times 10^{-5}$  days per period, which is much less than the period uncertainty adopted in this paper and in Lane et al. (2002).

Another unaccounted-for source of possible variations in the phase shift involves the possibility that the interferometric angular diameter may be slightly different (and off-phase) from the radius obtained by integrating the radial velocity measured from spectral lines. This discrepancy is mostly taken into account by the  $p$ -factor, but there may be unaccounted-for effects introducing an extra phase lag. Finally, even though the period may be stable for better than  $10^{-4}$  days per cycle, there may still be a variable phase shift between maximum light and minimum radius, causing a drift of the  $\Delta R(\phi_V)/D$  curve with respect to the light-curve phase  $\phi_L$ . This is a possibility that could affect the phase-dependent quantities involved in the calculations using the BW method, among which are the projection factor  $p(\phi)$  and the LD correction derived from

hydrodynamic models, which require the exact knowledge of the phase relation between models (computed in terms of the dynamical phase) and observations (dependent on the light-curve phase). There are no indications, however, that such an effect is present. Our best-fit results in Table 1, in fact, suggest that the uncertainty in the phase shift affects the best-fit diameter for only less than 0.001 mas, which is less than 1% of the estimated amplitude of the  $\zeta$  Gem pulsation. This error is small enough to be ignored when applying the BW method, compared with the other larger uncertainties in the data.

These considerations suggest that, given the current accuracy of interferometric data, we are not in a position to provide an independent measurement of the phase shift with better quality than the available data from Bersier et al. (1994a, 1994b). The effect measured with the independent fit is very small and does not significantly affect the fit of  $R_0$  and  $D$ . For these reasons we conclude that a two-parameter fit for the BW method is currently preferable to leaving the phase shift as a third free parameter.

However, we note that possible variations in the maximum luminosity–minimum radius phase shift should be taken into consideration when the precision of interferometric measurements and the accumulation of good-quality data over a long period of time make their direct observation feasible. Even though unpredicted phase shifts may appear unlikely with our current data, their possible occurrence should be monitored, as they can provide important insights into the mechanics of pulsations and their relation for stellar evolution.

### 3.2. Limb Darkening

The remaining question concerning the accuracy of the BW fit involves the LD. The LD correction is necessary in order to take into account the nonuniform brightness of the stellar disk, resulting from the different depths in the stellar atmosphere probed by different lines of sight. When a star is partially resolved by interferometric observations, the existence of LD induces a change in the measured visibility with respect to the simpler case of a uniform-brightness disk. The translation of interferometric visibilities into angular diameters takes into account this effect by fitting the data with limb-darkened model visibilities. Alternatively, when the original data have already been fitted with a UD model, an LD correction can be applied.

As in the case of the  $p$ -factor, the LD corrections can be obtained by solving the dynamic structure of the pulsating stellar atmosphere and then computing a complete radiative transfer model to derive the center-to-limb intensity profile. By using this approach we have derived a method to compute LD profiles for pulsating Cepheids, presented in Paper I. We have then computed specific phase- and wavelength-dependent LD corrections for  $\zeta$  Gem, taking into account second-order accurate one-dimensional hydrodynamic calculations performed in spherical geometry and a full set of atomic and molecular opacities (Marengo et al. 2003, hereafter Paper II).

To convert the UD diameters  $\theta_i^{(UD)}$  used in the previous section into the LD ones, one has to divide by the LD correction  $k(\lambda, \phi)$ :

$$\theta_i^{(LD)} = \frac{\theta_i^{(UD)}}{k(\lambda, \phi)}. \quad (15)$$

Figure 3 shows the LD corrections we presented in Paper II for  $\zeta$  Gem. The top curve shows  $k$  as a function of the pulsational phase for the PTI  $H$  band. The model LD correction

TABLE 1  
BW BEST FIT OF  $\zeta$  GEM PTI  $H$ -BAND UD DATA

Parameter	Fixed $\Delta\phi$	Free $\Delta\phi$
$\Delta\phi$ .....	0.280	0.294
$R_0$ ( $R_\odot$ ).....	$66.1^{+8.6}_{-6.8}$	$66.2^{+8.6}_{-6.8}$
$D$ (pc).....	$375^{+49}_{-39}$	$376^{+49}_{-39}$
$\Theta_0$ (mas).....	$1.630 \pm 0.007$	$1.629 \pm 0.007$

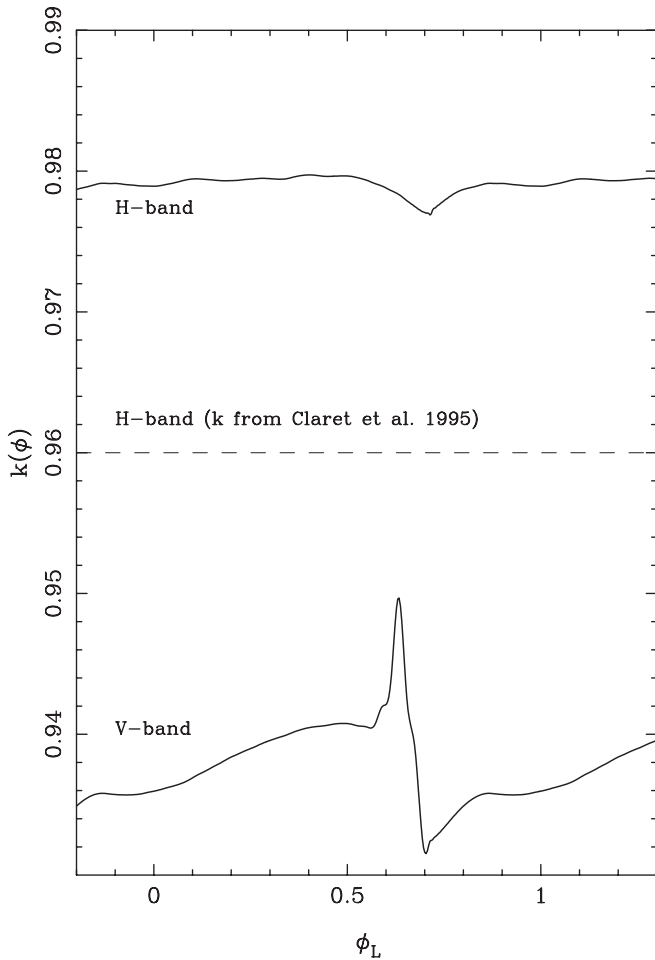


FIG. 3.—Phase-dependent LD corrections for  $\zeta$  Gem computed by the model presented in Paper II. The LD correction is shown for the PTI  $H$  band in the near-IR, and for the optical  $V$  band.

does indeed change with phase, with a  $\pm 0.3\%$  variation around the average value  $\bar{k} = 0.979$ . The largest change occurs close to minimum radius, when a shock wave crosses the Cepheid atmosphere (see Paper I). Barring systematic errors in our models, we can assume the uncertainty in the phase dependence as the total error on our LD correction estimate. From Paper II we have that this uncertainty results in an extra error of  $\sigma_i^{(\text{LD})} \simeq 0.003$  mas ( $\sim 3\%$  of the  $\zeta$  Gem pulsational amplitude), which is small with respect to the interferometric data errors. The BW distance computed with this correction is shown in Figure 4 and in Table 2. For comparison we have also solved the  $\zeta$  Gem BW fit using the LD correction  $k \simeq 0.96 \pm 0.01$  (Fig. 3, *dashed line*), derived from tabulated values computed by Claret, Díaz-Cordovéz, & Giménez (1995) for static yellow supergiants. This values have been used by Lane et al. (2002) to derive the PTI BW distance for  $\zeta$  Gem published in their paper. Given the quoted uncertainty, this results in an extra error source of  $\sigma_i^{(\text{LD})} \simeq 0.02$  mas (as much as 20% of the pulsational amplitude).

Figure 4 shows that, within the quoted error uncertainties, the two solutions for the BW fit with different LD correction are mutually exclusive, as the respective  $1\sigma$  error regions do not intersect. In fact, the two LD solutions are also separate from the BW distance computed for UD diameters. This shows that even if the final error range in the best-fit  $R_0$  and  $D$  includes all three solutions, interferometric techniques could

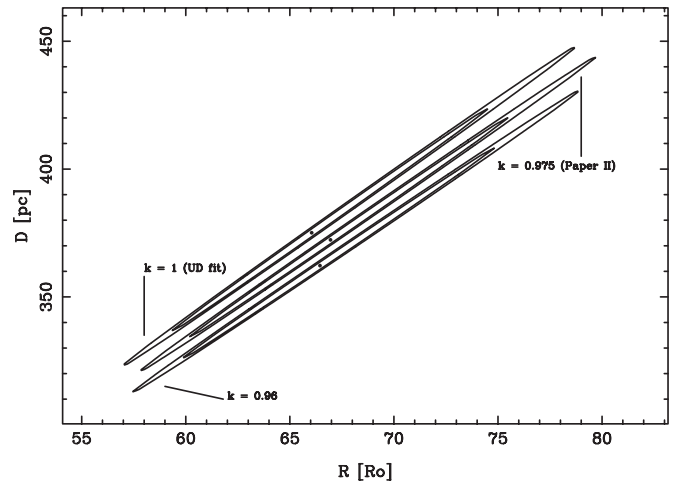


FIG. 4.—Best-fit parameters and error regions for  $\zeta$  Gem PTI  $H$ -band data. The top curve is the UD data, the middle curve is our best fit for model LD data, and the bottom curve is the result obtained using a fixed LD correction of  $k \simeq 0.96$  as in Lane et al. (2002). The inner region is the 68% confidence level of the fit ( $1\sigma$ ), while the outer is the 90% confidence level.

be used to discriminate between different models of LD. Alternatively, this result can be seen as an indication of how an independent determination of the LD will result in a much better measurement of pulsating star distance with the BW method.

#### 4. DISCUSSION AND CONCLUSIONS

Table 3 summarizes the error balance of the geometric BW method. For each error source, the table provides the resulting uncertainty in the determination of the Cepheid angular diameter in milliarcseconds and as a fraction of the  $\zeta$  Gem 0.1 mas pulsation amplitude. The last column of the table shows how these uncertainties affect the final determination of the BW distance. The statistical error in the interferometric data is still the main source of error in the method, leading to the final  $1\sigma$  error bars of  $\sim 14\%$  in our fit. The systematic errors (related to the radial velocity and phase shift measurements, the  $p$ -factor, and the limb darkening) still play a secondary role. Note that the effect of the relative uncertainty of the systematic error sources, which we have estimated for the *amplitude* of the stellar pulsation, should be scaled down by roughly 1 order of magnitude to estimate their effect on the best-fit distance, since the BW distance depends on the stellar *radius*, which is more than 10 times larger than the pulsation amplitude.

The second error source in importance is the determination of the average value of the LD correction. The difference between the best-fit value of the BW distance obtained with our  $\zeta$  Gem model and with the LD coefficient derived by Claret et al. (1995) is  $\sim 3\%$ . Our  $\zeta$  Gem fit shows that using an LD correction that is not appropriate for the observed Cepheid can introduce an error as large as when not using LD at all

TABLE 2  
BW BEST FIT OF  $\zeta$  GEM PTI  $H$ -BAND LD DATA

Parameter	$k = 0.979$	$k = 0.96$
$R_0 (R_\odot)$ .....	$67.0^{+8.7}_{-6.9}$	$66.5^{+8.5}_{-6.7}$
$D$ (pc).....	$372^{+49}_{-39}$	$362^{+47}_{-37}$
$\Theta_0$ (mas).....	$1.665 \pm 0.007$	$1.699 \pm 0.007$

TABLE 3  
INDIVIDUAL ERROR CONTRIBUTIONS SUMMARY

Error Source	$\sigma$ (mas)	$\zeta$ Gem Amplitude (%)	BW Distance (%)
$\theta_i$ measurement .....	0.01–0.06	10–60	14
Radial velocity .....	0.002	2	0.2
$p$ -factor .....	0.004	4	0.4
Phase shift .....	<0.001	<1	<0.1
LD average value .....	0.02	20	2
LD phase variations (H band) .....	<0.003	<3	<0.3
LD phase variations (B band) .....	<0.02	<20	<2

(e.g., using a UD model). This stresses the importance of reliable modeling of the Cepheid atmosphere even when using interferometric data with the currently best available quality.

The table also shows that the uncertainties in the radial velocity, phase shift,  $p$ -factor, and phase dependence of the LD correction at near-IR wavelength all together are responsible for less than a 1% error in the BW distance determination. These uncertainties play only a secondary role compared with the measurement errors. However, with the constant progress in the development of the interferometric techniques, the visibility errors are bound to be reduced, and at that point these other factors, as discussed above, will become essential to fulfill the potential of the BW method. This will be especially true for interferometers operating at visible wavelengths. Figure 3 shows the LD correction we have computed for  $\zeta$  Gem with our model in the  $V$  band (*bottom solid line*). The plot suggests that at certain phases in which the hydrodynamic effects play an important role (close to minimum radius and in the presence of shock waves) the interferometric measurement of the Cepheid pulsation amplitude can be affected by as much as 20%. This may result in a further uncertainty of up to 2% in the BW distance determination, which can be corrected only with an accurate time-dependent hydrodynamic modeling of the Cepheid atmosphere.

Even considering all the error sources discussed in the previous sections, the current error bar for the  $\zeta$  Gem BW diameter is already twice as good as the quoted error in parallax measurements for this star, which is  $\sim 30\%$  (*Hipparcos*; ESA 1997). A careful analysis of the error regions in the best-fit plane

shows that the error in the best-fit angular diameter is in fact much smaller than the individual errors in  $R_0$  and  $D$ , leaving room for dramatic improvements in the distance measurement if independent constraints are set on the stellar radius. These can be derived by modeling the structure of the pulsating atmosphere.

The results presented in this work show that a better determination of the limb darkening of the pulsating star can already lead to different estimates of the distance and average radius that are mutually exclusive. This justifies the recent efforts in producing accurate predictions for the model-dependent quantities needed by the BW method, by means of detailed self-consistent hydrodynamic models of the pulsating atmosphere (see, e.g., Papers I and II). An independent determination of the LD correction for nearby pulsating stars, which will be attainable once interferometers with baselines of several hundred meters become operative, will thus provide a direct test for such models. This will open the road for a large-scale application of the geometric BW method to derive the distances of a large sample of pulsating stars and thus attain the goal of an accurate calibration of their PL relation.

We wish to thank the anonymous referee for comments that helped us to improve this paper. This work was partially supported by NSF grant AST 98-76734. M. K. is a member of the Chandra Science Center, which is operated under contract NAS8-39073, and is partially supported by NASA.

## REFERENCES

- Baade, W. 1926, *Astron. Nachr.*, 228, 359  
 Balog, Z., Vinkó, J., & Kaszás, G. 1997, *AJ*, 113, 1833  
 Berdnikov, L. N., Ignatova, V. V., Caldwell, J. A. R., & Koen, C. 2000, *NewA*, 4, 625  
 Bersier, D., Burki, G., & Burnet, M. 1994a, *A&AS*, 108, 9  
 Bersier, D., Burki, G., Mayor, M., & Duquennoy, A. 1994b, *A&AS*, 108, 25  
 Böhm-Vitense, E., Garnavich, P., Lawler, M., Mena-Werth, J., Morgan, S., Peterson, E., & Temple, S. 1989, *ApJ*, 343, 343  
 Bono, G., Caputo, F., & Stellingwerf, R. F. 1994, *ApJ*, 432, L51  
 Cacciari, C., Clementini, G., & Fernley, J. A. 1992, *ApJ*, 396, 219  
 Claret, A., Díaz-Cordovéz, J., & Giménez, A. 1995, *A&AS*, 114, 247  
 ESA. 1997, *The Hipparcos and Tycho Catalogues* (ESA SP-1200; Noordwijk; ESA)  
 Feast, M. W., & Catchpole, R. M. 1997, *MNRAS*, 286, L1  
 Fernley, J. 1994, *A&A*, 284, L16  
 Frodesen, A. G., Skjeggstad, O., & Tofte, H. 1979, *Probability and Statistics in Particle Physics* (Bergen: Universitetsforlaget)  
 Gautschy, A. 1997, *Vistas Astron.*, 30, 197  
 Gieren, W. P., Barnes, T. G., & Moffett, T. J. 1993, *ApJ*, 418, 135  
 Jones, R. V., Carney, B. W., Storm, J., & Latham, D. W. 1992, *ApJ*, 386, 646  
 Kervella, P., Coudé du Foresto, V., Perrin, G., Schöller, M., Traub, W. A., & Lacasse, M. G. 2001, *A&A*, 367, 876  
 Krockenberger, M., Sasselov, D. D., & Noyes, R. W. 1997, *ApJ*, 479, 875  
 Lane, B. F., Creech-Eakman, M., & Nordgren, T. 2002, *ApJ*, 573, 330  
 Lane, B. F., Kuchner, M. J., Boden, A. F., Creech-Eakman, M., & Kulkarni, S. R. 2000, *Nature*, 407, 485  
 Laney, C. D., & Stobie, R. S. 1995, *MNRAS*, 274, 337  
 Marengo, M., Karovska, M., Sasselov, D., Papiolios, C., Armstrong, T., & Nordgren, T. 2003, *ApJ*, 589, 968 (Paper II)  
 Marengo, M., Sasselov, D. D., Karovska, M., Papiolios, C., & Armstrong, J. T. 2002, *ApJ*, 567, 1131 (Paper I)  
 McDonald, L. H. 1977, Ph.D. thesis, Univ. California, Santa Cruz  
 Meylan, G., Burki, G., Rufener, M., Mayor, M., Burnet, M., & Ischi, E. 1986, *A&AS*, 64, 25  
 Ripepi, V., Barone, F., Milano, L., & Russo, G. 1997, *A&A*, 318, 797  
 Sabbey, C. N., Sasselov, D. D., Fieldus, M. S., Lester, J. B., Venn, K. A., & Butler, R. P. 1995, *ApJ*, 446, 250  
 Sasselov, D. D., & Karovska, M. 1994, *ApJ*, 432, 367  
 Weselink, A. 1946, *Bull. Astron. Inst. Netherlands*, 10, 91